

# Nonlinear Rosseland thermal radiation and magnetic field effects on flow and heat transfer over a moving surface with variable thickness in a nanofluid

Mohamed S. Abdel-wahed

**Abstract:** A numerical investigation has been done to study the impact of nonlinear magnetic field, nonlinear thermal radiation, variable thickness, and Brownian motion on flow and heat transfer characteristics (i.e., skin friction and surface heat flux) as a physical application. Moreover, the impact of these forces on the rate of cooling and the mechanical properties (i.e., hardness, ductility, ...) of a surface that is cooled using nanofluid as a coolant is explored. The governing boundary layer equations describing the problem are transformed to ordinary differential equations using the similarity transformation method and are then solved numerically using the fourth-order Runge-Kutta method with shooting technique with the assistance of Mathematica program.

**Key words:** nanofluids, variable thickness, nonlinear thermal radiation, magnetic field.

**Résumé :** Nous présentons une étude numérique de l'impact d'un champ magnétique non linéaire, de la radiation thermique non linéaire, de l'épaisseur variable et du mouvement brownien sur les caractéristiques d'écoulement et de transfert de chaleur (i.e. le frottement superficiel et le flux de chaleur de surface) en tant que un système physique. Nous étudions aussi l'impact de ces forces sur le taux de refroidissement et les propriétés mécaniques (i.e., la dureté, la ductilité, ...) des surfaces refroidies en utilisant un nanofluide comme refroidisseur. Les équations directrices de la couche limite sont transformées en en équations différentielles ordinaires par la méthode des transformations de similarité, qui sont ensuite solutionnées par méthode de Runge-Kutta du quatrième ordre avec une technique de tir en utilisant un programme de Mathematica. [Traduit par la Rédaction]

**Mots-clés :** nanofluide, épaisseur variable, radiation thermique non linéaire, champ magnétique.

## 1. Introduction

Study of boundary layer behavior over a moving surface is an important problem because of its importance to industry processes, such as paper production, plastic extrusion, and fibers. This is not the only application of the problem. Moreover, it is considered as a mathematical simulation to the heat treatment processes of the metal surfaces that are subjected to an increase in temperature and cooling to reach to the required mechanical properties.

The boundary layer flow caused by a moving surface has drawn the attention of many researches [1–13]. Through these papers, the researchers have become interested in some external forces acting on the boundary layer, such as magnetic field, thermal radiation, heat generation, suction-injection process, and the unsteady motion. The concept of using a regular fluid for cooling has been changed after defining a new type of fluid called a nanofluid by Choi [14].

Choi defined a new type of fluid consisting of suspended particles of nano size within a regular fluid, such as oil, water, or ethylene glycol. These particles improve the thermal conductivity of the flow, which opens new and wide applications in the industry, especially in the field of cooling and heat treatment processes.

The behavior of the nanofluid boundary layer over a moving surface was investigated by Rohni et al. [15], who studied the effect of unsteady motion of a shrinking sheet in the presence of suction.

Rana et al. [16] studied the effect of nonlinear velocity of a stretching sheet in nanofluids. Aminreza et al. [17] investigate the effect of partial slip boundary condition on the flow and heat transfer of nanofluids past a stretching surface with constant wall temperature. Hamad [18] presented an analytical solution for natural convection flow of nanofluids with magnetic field. Yacob et al. [19] studied the effect of external uniform shear flow with convective surface boundary condition on a nanofluid over a shrinking surface. Elbashbeshy et al. [20, 21] deduced an exact solution to the nanofluid boundary layer problem over a moving surface in the presence of magnetic field and suction-injection process for both steady and unsteady motion. The effect of heat generation on the thermal boundary layer of a nanofluid was studied by Alsaedi et al. [22].

The effect of thermal radiation on the nanofluid boundary for different cases was investigated by Magyari et al. [23], Motsumi et al. [24], Hady [25], Elbashbeshy et al. [26], Pantokratoras and Fang [27], Mohyud-Din et al. [28], Khan et al. [29], and Abdel-wahed et al. [30, 31].

It is worth mentioning that all previous papers considered a uniform distribution of nanoparticles within the boundary layer. The effect of Brownian motion and thermophoresis on the nanoparticles' distribution within the boundary layer was investigated by Anbucuzhan et al. [32] and Kandasamy et al. [33].

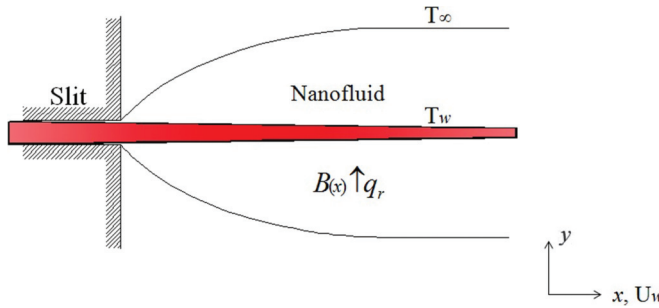
Variable thickness may occur in engineering applications more frequently than a flat surface. Fang et al. [34], Elbashbeshy et al.

Received 19 May 2016. Accepted 1 December 2016.

**M.S. Abdel-wahed.** Basic Sciences Department, Faculty of Engineering at Benha, Benha University, Cairo, Egypt.

**Email for correspondence:** eng\_moh\_sayed@live.com.

Copyright remains with the author(s) or their institution(s). Permission for reuse (free in most cases) can be obtained from RightsLink.

**Fig. 1.** Physical model and coordinate system. [Colour online.]

[35], and Abdel-wahed et al. [36] developed the study of the boundary layer problem by taking into consideration the effect of the surface thickness variation on the boundary layer behavior in the presence of different forces.

The present work investigates the effect of nonlinear Rosseland thermal radiation and nonlinear magnetic field on the boundary layer behavior and the impact of these forces on the mechanical properties of a surface with variable thickness through the process of cooling.

## 2. Formulation of the problem

It is assumed that a surface with variable thickness  $y = \delta(x + b)^{(1-n)/2}$  moving with nonlinear velocity  $U_w(x) = a(x + b)^n$  within a steady, laminar, incompressible cooling medium consists of nanoparticles and water base fluid. The fluid subjected to nonlinear transverse magnetic field with strength of  $B(x) = B_0(x + b)^{(n-1)/2}$  and nonlinear thermal radiation with heat flux  $q_r = -(4\sigma^*/3\sigma^*)(\partial T^4/\partial y)$ .

Moreover, it is assumed that the surface is sufficiently thin with no induced stream-wise pressure gradients and the induced magnetic field produced by the motion of an electrically conducting fluid is negligible.

As shown in Fig. 1, the temperature of the surface assumed  $T_w$  and the ambient temperature of the boundary layer taken  $T_\infty$ .

The governing boundary layer equations describing the steady two-dimensional laminar hydromagnetic nanofluid flow over a moving surface and subjected nonlinear Rosseland thermal radiation can be written as

$$\frac{\partial u}{\partial x} + \frac{\partial v}{\partial y} = 0 \quad (1)$$

$$u \frac{\partial u}{\partial x} + v \frac{\partial u}{\partial y} = \nu \frac{\partial^2 u}{\partial y^2} - \frac{\sigma B^2(x)}{\rho} u \quad (2)$$

$$u \frac{\partial T}{\partial x} + v \frac{\partial T}{\partial y} = \alpha^* \frac{\partial^2 T}{\partial y^2} + \tau \left[ D_B \frac{\partial C}{\partial y} \frac{\partial T}{\partial y} + \frac{D_T}{T_\infty} \left( \frac{\partial T}{\partial y} \right)^2 \right] + \left( \frac{4\sigma^*}{3\alpha^* \rho C_p} \right) \frac{\partial^2 T^4}{\partial y^2} \quad (3)$$

$$u \frac{\partial C}{\partial x} + v \frac{\partial C}{\partial y} = D_B \frac{\partial^2 C}{\partial y^2} + \frac{D_T}{T_\infty} \left( \frac{\partial^2 T}{\partial y^2} \right) \quad (4)$$

With boundary conditions

$$\begin{aligned} u &= U_w & v &= 0 & T &= T_w & C &= C_w \\ \text{at } y &= \delta(x + b)^{(1-n/2)} & u &= 0 & v &= 0 & T &= T_\infty & C &= C_\infty \\ \text{as } y &\rightarrow \infty & & & & & & & \end{aligned} \quad (5)$$

Where  $n$  is the shape parameter. It is assumed  $n > -1$  in this work for the validity of the similarity variable and functions.

## 3. Similarity transformation

We are looking for a similarity solution of (1)–(4) with boundary conditions (5) using the following form:

$$\eta = y \sqrt{\left( \frac{n+1}{2} \right) \left[ \frac{a(x+b)^{n-1}}{v} \right]} \quad \psi = \sqrt{\left( \frac{2}{n+1} \right) (x+b)^{n+1} a \psi(\eta)} \quad (6)$$

Assuming the boundary layer temperature and nanoparticle concentration take the form

$$T = T_\infty + (T_w - T_\infty) \theta(\eta) \quad \text{and} \quad C = C_\infty + (C_w - C_\infty) \phi(\eta) \quad (7)$$

where  $\eta$  is the similarity variable and  $\psi$  is the stream function, which is defined as  $u = \partial \psi / \partial y$  and  $v = \partial \psi / \partial x$ , which satisfies (1).

Substituting (6) into (2)–(4), one can obtain the following ordinary differential equations:

$$F''' + FF'' - \left( \frac{2n}{n+1} \right) F'^2 - \left( \frac{2}{n+1} \right) MF' = 0 \quad (8)$$

$$3\theta'' + R_d \frac{[1 + (\theta_w - 1)\theta]^4}{(\theta_w - 1)} + 3Pr \left( F\theta' + N_b \theta' \phi' + N_t \theta'^2 \right) = 0 \quad (9)$$

$$\phi'' + \frac{1}{2} Le F \phi' + \left( \frac{N_t}{N_b} \right) \theta'' = 0 \quad (10)$$

With boundary conditions

$$F(\alpha) = \alpha \left( \frac{1-n}{1+n} \right) \quad F'(\alpha) = 1 \quad \theta(0) = 1 \quad \phi(0) = 1 \quad \text{and} \quad (11)$$

$$F'(\infty) = 0 \quad \theta(\infty) = 0 \quad \phi(\infty) = 0$$

here primes denote differentiation with respect to  $\eta$ .

By defining  $F(\eta) = f(\eta - \alpha) = f(\zeta)$ , similarity equations (8)–(10) and associated boundary conditions (11) become

$$f''' + ff'' - \left( \frac{2n}{n+1} \right) f'^2 - \left( \frac{2}{n+1} \right) Mf' = 0 \quad (12)$$

$$\begin{aligned} \left\{ 1 + \frac{4R_d}{3} [1 + (\theta_w - 1)\theta]^3 \right\} \theta'' + 4R_d(\theta_w - 1)[1 + (\theta_w - 1)\theta]^2 \theta'^2 \\ + Pr \left( f\theta' + N_b \theta' \phi' + N_t \theta'^2 \right) = 0 \quad (13) \end{aligned}$$

$$\phi'' + \frac{1}{2} Le f \phi' + \left( \frac{N_t}{N_b} \right) \theta'' = 0 \quad (14)$$

With boundary conditions

$$f(0) = \alpha \left( \frac{1-n}{1+n} \right) \sqrt{\frac{1+n}{2}} \quad f'(0) = 1 \quad \theta(0) = 1 \quad \phi(0) = 1 \quad (15)$$

$$\text{and} \quad f'(\infty) = 0 \quad \theta(\infty) = 0 \quad \phi(\infty) = 0$$

here prime denotes differentiation with respect to  $\zeta$ .

## 4. Numerical solution

Using Mathematica, (12)–(14) with boundary conditions (15) are solved using the shooting method as a boundary value problem. In this process, it is necessary to choose a suitable finite value  $\zeta \rightarrow \infty$ , say  $\zeta_\infty$ . Moreover, we require values for  $f''(0)$ ,

**Table 1.** The values of  $-\theta'(0)$  at different values of  $\theta_w$  and  $R_d$  at  $Pr = 5.5$ .

$R_d$	$\theta_w$	Pantokratoras and Fang [27]	Present work
0.6	1.10	0.5338	0.5332
	1.50	0.3069	0.3067
	2.00	0.1708	0.1706
10	1.10	1.1053	1.1050
	1.50	0.9516	0.9513
	2.00	0.7358	0.7357

$\theta'(0)$ , and  $\phi'(0)$  but no such values are given in the problem. Suitable guess values for  $f''(0)$ ,  $\theta'(0)$ , and  $\phi'(0)$  are chosen and then integration is carried out, and we compare the calculated values for  $f''(0)$ ,  $\theta'(0)$ , and  $\phi'(0)$  at  $\zeta = \zeta_{\max} \equiv 100$  with the given boundary conditions  $f'(\zeta_\infty) = 0$ ,  $\theta(\zeta_\infty) = 0$ ,  $\phi(\zeta_\infty) = 0$ , and adjust the estimated values,  $f''(0)$ ,  $\theta'(0)$ , and  $\phi'(0)$  using the “secant method” to give a better approximation for the solution by taking a series of values for  $f''(0)$ ,  $\theta'(0)$ , and  $\phi'(0)$  and applying the fourth-order classical “Runge–Kutta method” with step size  $\Delta\zeta = 0.01$ . This procedure is repeated until we get the converged results within a tolerance limit of  $10^{-6}$ . To validate the accuracy of this method, the paper of Pantokratoras and Fang [27] was resolved by this method and the results obtained were compared with [27] and appear to be in good agreement (see Table 1).

## 5. Results

As mentioned before, the most important application of nanofluid is as a coolant because of its high thermal conductivity. One of these applications is a heat treatment process that aims to improve the mechanical properties of the surface by heating and cooling it in succession. The rate of cooling (heat flux) in this process controls the hardness, stiffness, strength, ductility, and surface cracking. So this work focuses on this point as well as other physical parameters, such as surface shear stress and the mass flux.

### 5.1. Surface shear stress

$$\tau_w = \mu \left( \frac{\partial u}{\partial y} \right)_{y=\delta(x+b)^{(1-n)/2}} = \mu U_w \sqrt{\frac{a(n+1)}{2}(x+b)^{n-1} f''(0)} \quad (16)$$

Because the skin friction coefficient is given by

$$C_f = \frac{2\tau_w}{\rho U_w^2} \quad \text{i.e.,} \quad 2\sqrt{\frac{n+1}{2}} f''(0) = \sqrt{R_e} C_{fx} \quad (17)$$

### 5.2. Surface heat flux (rate of heat transfer)

$$q_w = (q_r)_w - k \left( \frac{\partial T}{\partial y} \right)_{y=\delta(x+b)^{(1-n)/2}} = - \left[ k(T_w - T_\infty) \sqrt{\frac{n+1}{2}} \frac{a}{v} \right. \\ \times (x+b)^{(n-1)/2} + \left. \frac{4}{3} R_d k T_\infty (\theta_w - 1) \theta_w^3 \right] \theta'(0) \quad (18)$$

Because the Nusselt number is given by

$$Nu = \frac{(x+b)q_w}{k(T_w - T_\infty)} \quad \text{i.e.,} \quad Nu = - \left( \sqrt{\frac{n+1}{2}} \sqrt{R_e} + \frac{4R_d \theta_w^3}{3} \right) \theta'(0) \quad (19)$$

**Table 2.** Values of skin friction, Nusselt number, and Sherwood number at  $M = 0.5$ ,  $Le = 2$ ,  $Pr = 6.2$ ,  $N_t = N_b = 0.1$ ,  $\theta_w = 1.2$ , and  $R_d = 5$ .

$\alpha$	$n$	$f''(0)$	$\theta'(0)$	$\phi'(0)$	$C_{fx}$	$Nu$	$Sh$
0.5	-0.50	-1.538121	-1.675650	0.418655	-0.00218	596.29	-148.02
	1.00	-1.224745	-0.292469	-0.341444	-0.00346	207.48	241.44
	1.50	-1.182711	-0.260553	-0.305144	-0.00374	206.59	241.24
1	-0.50	-2.118823	-2.808684	0.931084	-0.00300	999.49	-329.19
	1.00	-1.224745	-0.292469	-0.341444	-0.00346	207.48	241.44
	1.50	-1.131429	-0.228266	-0.267573	-0.00358	180.99	211.53
2	-0.50	-3.413214	-5.229440	1.989354	-0.00483	1860.93	-703.34
	1.00	-1.224745	-0.292469	-0.341444	-0.00346	207.48	241.44
	1.50	-1.036347	-0.168802	-0.198050	-0.00328	133.84	156.57

### 5.3. Surface mass flux (rate of mass transfer)

$$q_m = -D_B \left( \frac{\partial C}{\partial y} \right)_{y=\delta(x+b)^{(1-n)/2}} \\ = -D_B (C_w - C_\infty) \sqrt{\frac{n+1}{2}} \frac{a}{v} (x+b)^{(n-1)/2} \phi'(0) \quad (20)$$

Because the Sherwood number is given by

$$Sh = \frac{(x+b)q_m}{D_B(C_w - C_\infty)} \quad \text{i.e.,} \quad \frac{Sh}{\sqrt{R_e}} = - \sqrt{\frac{n+1}{2}} \phi'(0) \quad (21)$$

## 6. Discussion

This study presents thickness variation as a new and important factor that controls the outer surface shape, type of motion, and the behavior of the boundary layer. The outer shape of the surface depends on the value of  $n$ , such that  $n = 1$  (dot-dashed line) reduced to a flat surface with constant thickness ( $\delta$ ), while  $n < 1$  (solid line) indicates a surface with increasing thickness. However,  $n > 1$  (dashed line) transformed to a surface with decreasing thickness.

Moreover, the value of  $n$  controls the boundary layer behavior such that for  $n = 1$  boundary condition (15) reduced to  $f(0) = 0$ , which indicates an impermeable surface, while for,  $n < 1$  the boundary condition becomes  $f(0) > 0$ , which indicates a suction process, and for  $n > 1$  the boundary condition becomes  $f(0) < 0$ , which indicates an injection process.

The aim of this section is to discuss these three cases under the effect of the nonlinear Rosseland thermal radiation and magnetic field in the presence of Brownian motion and thermophoresis. The surface shear stress, rate of cooling, and rate of mass transfer are investigated through Tables 2–5.

### 6.1. Influence of surface flatness

The influence of variation of the surface thickness on the boundary layer behavior appears through the thickness parameter ( $\alpha$ ). Figures 2, 3, and 4 present the velocity, temperature, and the concentration profiles as thickness parameter varies. It is observed that increasing  $\alpha$  leads to decreasing velocity, temperature, and nanoparticle concentration in the case of  $n < 1$  and the opposite is true for  $n > 1$  and no effect of thickness parameter on the boundary layer in the case of flat surface  $n = 0$ . Moreover, one can observe that the thermal and concentration boundary layer thickness in the case of  $n < 1$  is larger than that in the case of  $n > 1$ . In addition, it is clear that the concentration of nanoparticles close to the surface in the case  $n < 1$  is higher than that in the case  $n > 1$ .

On the other hand, Table 2 shows the effect of thickness parameter on the velocity gradient, temperature gradient, and the concentration gradient and the corresponding values of skin friction,

**Table 3.** Values of skin friction, Nusselt number, and Sherwood number at  $\alpha = 1$ ,  $Le = 2$ ,  $Pr = 6.2$ ,  $N_t = N_b = 0.1$ ,  $\theta_w = 1.2$ , and  $R_d = 1$ .

M	n	$f''(0)$	$\theta'(0)$	$\phi'(0)$	$C_{fx}$	Nu	Sh
0	-0.50	-1.166667	-2.842126	0.856815	-0.00165	1011.39	-302.93
	1.00	-1.000000	-0.324760	-0.385737	-0.00283	230.39	272.76
	1.50	-0.957891	-0.258670	-0.309025	-0.00303	205.09	244.31
0.5	-0.50	-2.118823	-2.808684	0.931084	-0.00300	997.51	-329.19
	1.00	-1.224745	-0.292469	-0.341444	-0.00346	207.48	241.44
	1.50	-1.131429	-0.228294	-0.267769	-0.00358	181.01	211.69
1	-0.50	-2.698243	-2.790261	0.963717	-0.00382	992.93	-340.73
	1.00	-1.414214	-0.268218	-0.310326	-0.00400	190.28	219.43
	1.50	-1.283263	-0.207393	-0.252124	-0.00406	164.44	199.32

**Table 4.** Values of skin friction, Nusselt number, and Sherwood number at  $\alpha = 1$ ,  $M = 0.5$ ,  $Le = 2$ ,  $Pr = 6.2$ ,  $N_t = N_b = 0.1$ , and  $\theta_w = 1.2$ .

$R_d$	n	$f''(0)$	$\theta'(0)$	$\phi'(0)$	$C_{fx}$	Nu	Sh
0.67	-0.50	-2.118823	-3.570320	1.679334	-0.00300	1274.64	-593.73
	1.00	-1.224745	-0.828226	0.070000	-0.00346	588.51	-49.50
	1.50	-1.131429	-0.538001	-0.075642	-0.00358	427.19	59.80
1	-0.50	-2.118823	-2.808684	0.931084	-0.00300	999.49	-329.19
	1.00	-1.224745	-0.709428	-0.027644	-0.00346	503.28	19.55
	1.50	-1.131429	-0.481856	-0.112276	-0.00358	382.05	88.76
5	-0.50	-2.118823	-0.843469	-0.963695	-0.00300	298.60	340.72
	1.00	-1.224745	-0.292469	-0.341444	-0.00346	206.94	241.44
	1.50	-1.131429	-0.228279	-0.267668	-0.00358	180.58	211.69

**Table 5.** Values of skin friction, Nusselt number, and Sherwood number at  $\alpha = 1$ ,  $M = 0.5$ ,  $Le = 2$ ,  $Pr = 6.2$ ,  $N_t = N_b = 0.1$ , and  $R_d = 0.8$ .

$\theta_w$	n	$f''(0)$	$\theta'(0)$	$\phi'(0)$	$C_{fx}$	Nu	Sh
1.2	-0.50	-2.118823	-0.843469	-0.963695	-0.00300	300.54	340.72
	1.00	-1.224745	-0.292469	-0.341444	-0.00346	207.62	241.44
	1.50	-1.131429	-0.228279	-0.267668	-0.00358	181.10	211.69
1.3	-0.50	-2.118823	-0.684537	-1.114219	-0.00300	244.43	393.94
	1.00	-1.224745	-0.244647	-0.376534	-0.00346	173.85	266.25
	1.50	-1.131429	-0.193244	-0.290079	-0.00358	153.45	229.33
1.4	-0.50	-2.118823	-0.562331	-1.228851	-0.00300	201.28	434.46
	1.00	-1.224745	-0.206251	-0.403629	-0.00346	146.75	285.41
	1.50	-1.131429	-0.164541	-0.307619	-0.00358	130.80	243.19
1.5	-0.50	-2.118823	-0.467004	-1.317470	-0.00300	167.63	465.80
	1.00	-1.224745	-0.175112	-0.424861	-0.00346	124.77	300.42
	1.50	-1.131429	-0.140860	-0.321560	-0.00358	112.12	254.22

Nusselt number, and Sherwood number. It noted that increasing the thickness parameter leads to an increase of all previous physical properties.

It is worth mentioning that increasing the rate of heat transfer from the surface leads to acceleration of the cooling process, which has a direct positive effect on surface mechanical properties of the surface, such as hardness, stiffness, and strength.

## 6.2. Influence of hydromagnetic flow

The effect of magnetic field on the boundary layer velocity, temperature, and concentration is shown through Figs. 5, 6, and 7. One can observe that the increase of magnetic parameter decreases the velocity and decreases the temperature and nanoparticle concentration. Moreover, it is clear that the effect of magnetic parameter on the temperature and nanoparticle concentration in the case of  $n < 1$  is very weak. In addition, with the same conditions, the nanoparticle concentration in the case of  $n < 1$  near the surface increases gradually and then decays to zero rapidly, unlike for the other  $n$ -values.

The effect of hydromagnetic flow on the skin friction, Nusselt number, and Sherwood number are tabulated in Table 3. By com-

**Fig. 2.** Velocity profiles with increasing thickness parameter ( $\alpha$ ). [Colour online.]

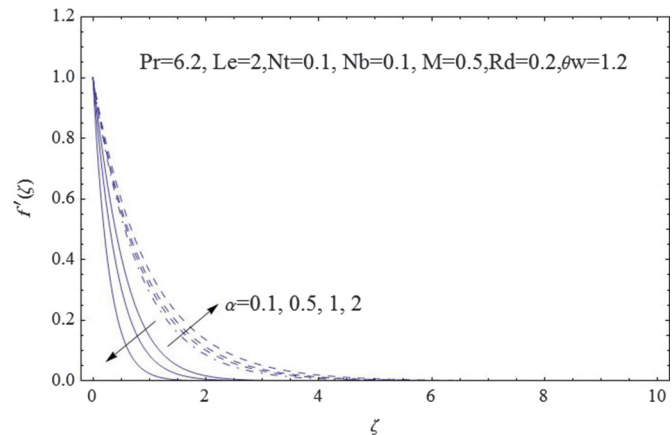


**Fig. 3.** Temperature profiles with increasing thickness parameter ( $\alpha$ ). [Colour online.]

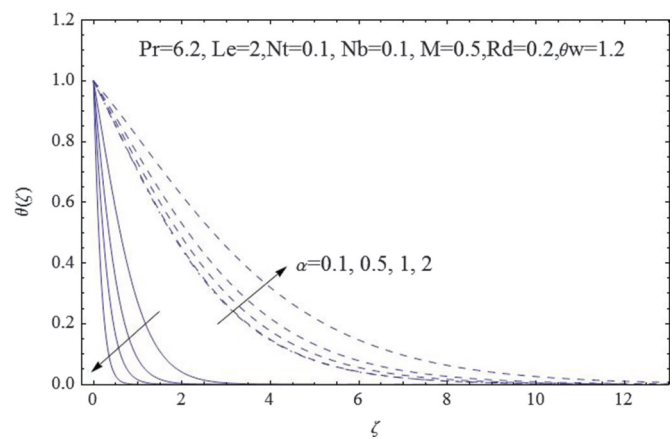
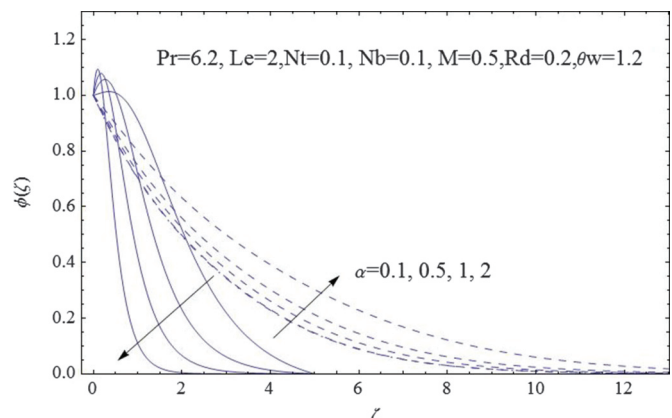


**Fig. 4.** Concentration profiles with increasing thickness parameter ( $\alpha$ ). [Colour online.]



paring, one can observe that using hydromagnetic flow as a cooling medium increase skin friction and Sherwood number and decreases Nusselt number. Consequently, the surface shear stress and rate of mass transfer increased and rate of heat transfer decreased by increasing magnetic parameter  $M$ .

**Fig. 5.** Velocity profiles with increasing magnetic parameter ( $M$ ). [Colour online.]

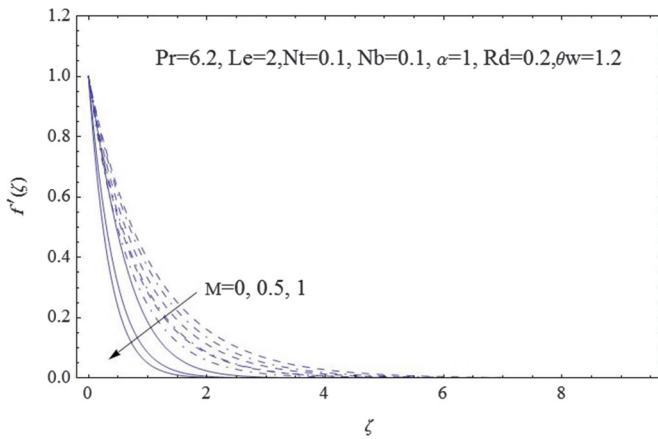


**Fig. 6.** Temperature profiles with increasing magnetic parameter ( $M$ ). [Colour online.]

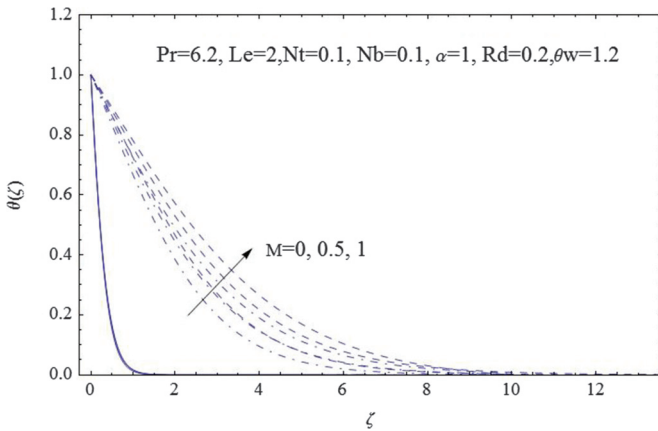
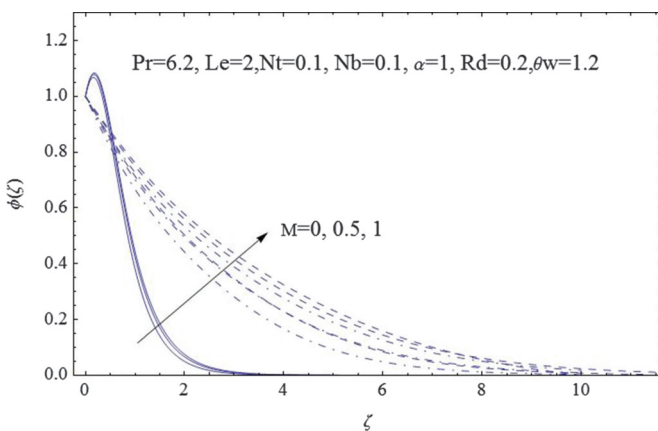


**Fig. 7.** Concentration profiles with increasing magnetic parameter ( $M$ ). [Colour online.]



### 6.3. Influence of nonlinear thermal radiation

The most recent papers investigate the effect of thermal radiation on the boundary layer through the linear Rosseland approximation, which appears in the dimensionless system through the radiation parameter ( $R_d$ ). One of this paper's goals is to study the effect of the thermal radiation through the nonlinear Ros-

**Fig. 8.** Temperature profiles with increasing radiation parameter ( $R_d$ ). [Colour online.]

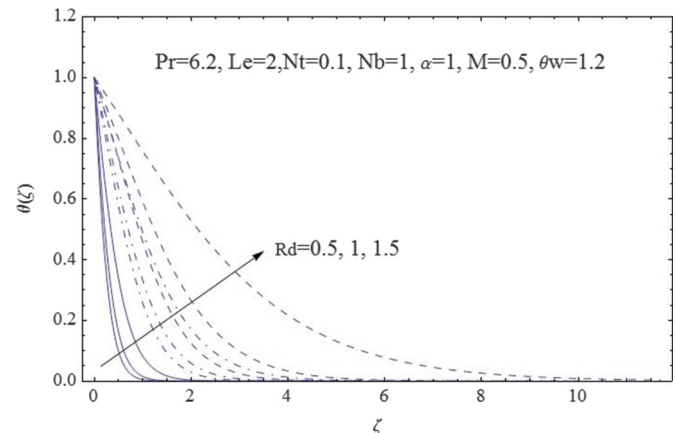
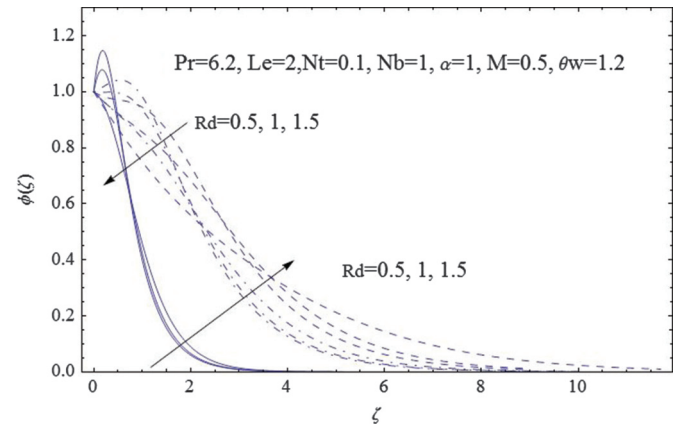


**Fig. 9.** Concentration profiles with increasing radiation parameter ( $R_d$ ). [Colour online.]



land approximation, which appears in the dimensionless system through the radiation parameter ( $R_d$ ) and temperature ratio parameter ( $\theta_w$ ).

The effect of the radiation parameter on the boundary layer temperature and concentration is plotted in Figs. 8 and 9. It is clear that the increase of this parameter increases the boundary layer temperature. In addition, one can observe that the impact of this parameter is more active when increasing its value. Moreover, the effect of the radiation parameter on the nanoparticle concentration is very clear, especially in the case of  $n > 1$ , such that its increase decreases the concentration near the surface before decaying to zero.

On the other hand, the effect of temperature ratio on the boundary layer temperature and concentration is shown by Figs. 10 and 11. The figures show that the increase of the temperature ratio increases the boundary layer temperature and decreases the concentration of the nanoparticles near the surface. Moreover, it is clear that at a certain zone in the boundary layer, the concentration is constant at any value of temperature ratio.

The effect of nonlinear radiation on the skin friction, Nusselt number, and Sherwood number is shown in Tables 4 and 5. It is clear that the presence of thermal radiation increases the temperature and the concentration gradient at the surface, which increases the Nusselt and Sherwood numbers. The same effect on the Sherwood number appears in the presence of temperature ratio parameter and the opposite is true for Nusselt number.

**Fig. 10.** Temperature profiles with increasing temperature ratio ( $\theta_w$ ). [Colour online.]

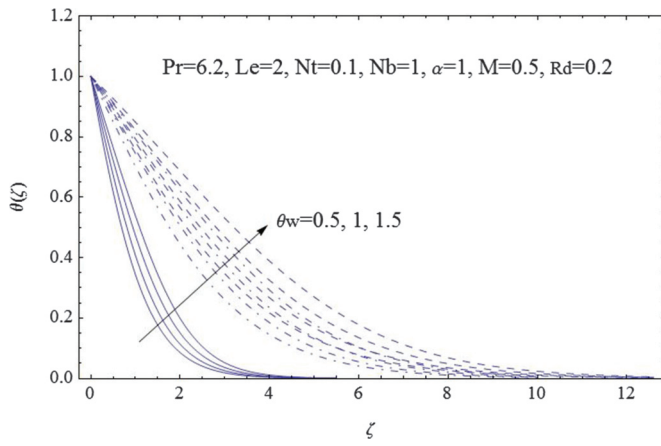


**Fig. 11.** Concentration profiles with increasing temperature ratio ( $\theta_w$ ). [Colour online.]

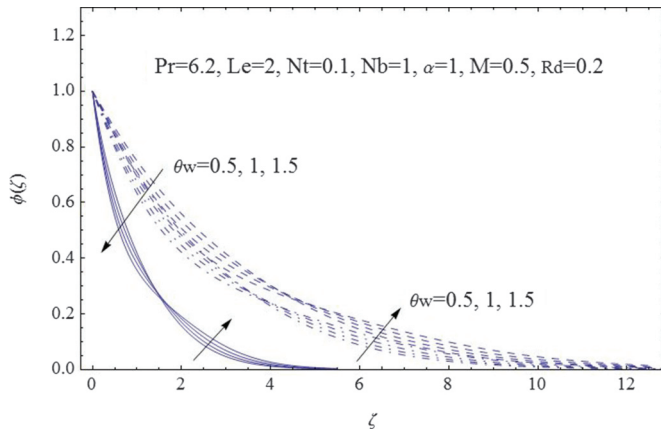
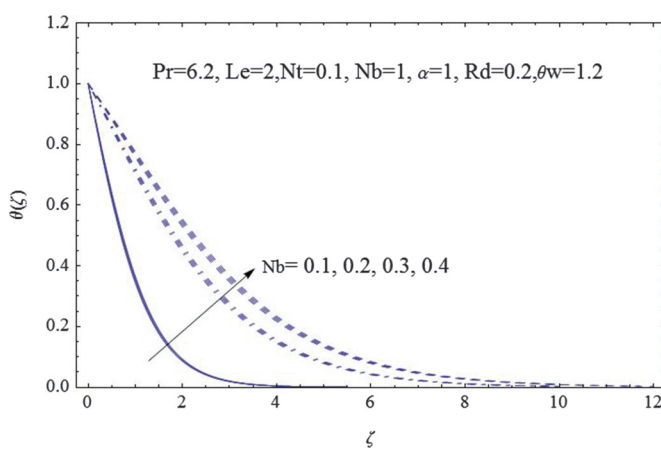


**Fig. 12.** Temperature profiles with increasing Brownian parameter  $N_b$ . [Colour online.]



#### 6.4. Influence of Brownian motion

The random movement of the particles suspended in a fluid (nanoparticles) resulting from their bombardment by fast-moving atoms or molecules in the fluid is called Brownian motion. This motion controls the temperature and the concentration of the particles within the boundary layer over the surface. The Brown-

**Fig. 13.** Concentration profiles with increasing Brownian parameter  $N_b$ . [Colour online.]

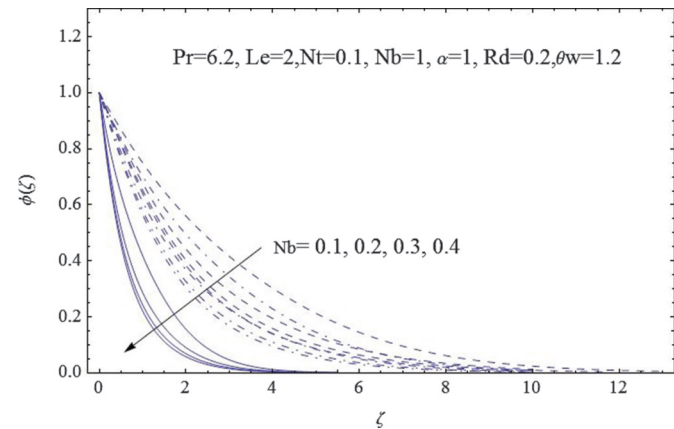


**Fig. 14.** Temperature profiles with increasing thermophoresis parameter  $N_t$ . [Colour online.]

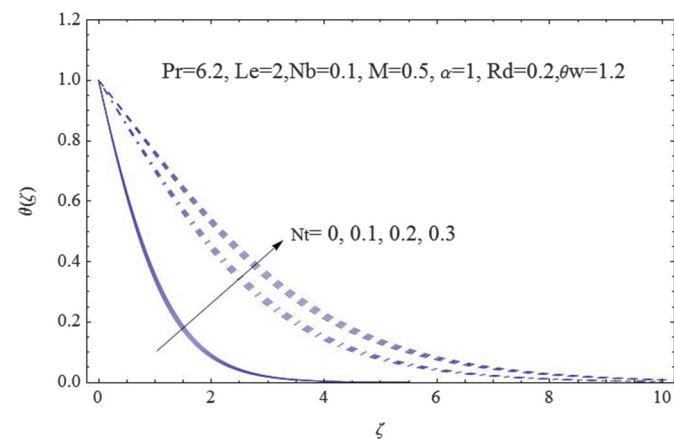
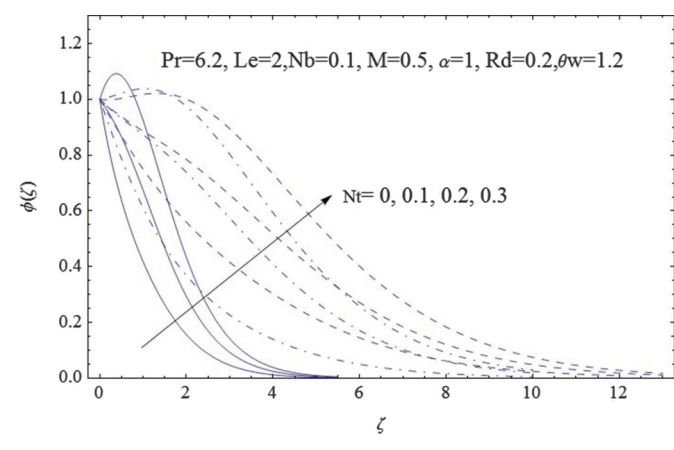


**Fig. 15.** Concentration profiles with increasing thermophoresis parameter  $N_t$ . [Colour online.]



ian motion parameter  $N_b$  is the key to this mechanism in this study, such that the increasing of  $N_b$  leads to increasing of the boundary layer temperature and decreasing of the nanoparticles concentration, as shown in Figs. 12 and 13. Moreover, it is clear that the impact of the random movement of particles on the

concentration decreases by increase the value of Brownian motion parameter for all values of shape parameter  $n$ .

### 6.5. Influence of thermophoresis particle deposition

Thermophoresis is a phenomenon observed in mixtures of mobile particles, where the different particle types exhibit different responses to the force of a temperature gradient. Influence of this phenomenon appears in this study through the thermophoresis parameter  $N_t$  such that increasing this parameter leads to increasing of boundary layer temperature and nanoparticle concentration, as shown in Figs. 14 and 15. In addition, Fig. 15 shows that the effect of this phenomenon on the concentration is more clear in the case of  $n > 1$ .

## 7. Conclusion

This study presents a mathematical model of a continuous moving surface with variable thickness embedded into a nanofluid under the effect of nonlinear thermal radiation and magnetic field. The behavior of the boundary layer under the suggested forces and the influence of these on the heat and mass transfer characteristics and the mechanical properties of the surface were the goal in this study and the following results were obtained:

- Thickness parameter ( $\alpha$ ) and shape parameter ( $n$ ) both play an important role in the thermal and concentration boundary layer behavior.
- The boundary layer thickness in the case of  $n < 1$  is bigger than that in the case of  $n > 1$ .
- Hydromagnetic flow has no strong effect on the boundary layer temperature and concentration in the case of  $n < 1$ .
- The nonlinear Rosseland thermal radiation has a clear impact on the thermal and concentration boundary layer.
- The Brownian motion and thermophoresis both have a clear impact on the nanoparticle concentration especially in the case of  $n > 1$ .
- The rate of heat transfer from the surface (Nusselt number) increases in the presence of thickness and radiation parameters and the opposite is true for magnetic and temperature ratio parameters.
- Generally, the rate of heat transfer from the convex outer shape surface ( $n < 1$ ) is higher than that in the case of concave outer shape surface ( $n > 1$ ).

## References

- M.E. Ali. Int. J. Heat Fluid Flow. **16**, 280 (1995). doi:[10.1016/0142-727X\(95\)00001-7](https://doi.org/10.1016/0142-727X(95)00001-7).
- E.M.A. Elbashbeshy and M.A.A. Bazid. J. Phys. D, Phys. **33**, 2721, (2000). doi:[10.1088/0022-3727/33/21/309](https://doi.org/10.1088/0022-3727/33/21/309).
- E.M.A. Elbashbeshy and M.A.A. Bazid. Appl. Math. Comput. **158**(3), 799 (2004). doi:[10.1016/j.amc.2003.08.141](https://doi.org/10.1016/j.amc.2003.08.141).
- E.M.A. Elbashbeshy and M.A.A. Bazid. Int. J. Heat Mass Trans. **43**, 3087 (2000). doi:[10.1016/S0017-9310\(99\)00359-2](https://doi.org/10.1016/S0017-9310(99)00359-2).
- E.M.A. Elbashbeshy and M.A.A. Bazid. Heat Mass Trans. **41**, 1 (2004). doi:[10.1007/s00231-004-0520-x](https://doi.org/10.1007/s00231-004-0520-x).
- E.M.A. Elbashbeshy and M.A.A. Bazid. Appl. Math. Comput. **138**(3), 239 (2003). doi:[10.1016/S0096-3003\(02\)00106-6](https://doi.org/10.1016/S0096-3003(02)00106-6).
- R. Nazar, N. Amin, I. Pop, and D. Flip. Int. J. Eng. Sci. **42**, 1241 (2004). doi:[10.1016/j.ijengsci.2003.12.002](https://doi.org/10.1016/j.ijengsci.2003.12.002).
- A. Ishak, R. Nazar, and I. Pop. Nonlinear Anal.: Real World Appl. **10**, 2909 (2009). doi:[10.1016/j.nonrwa.2008.09.010](https://doi.org/10.1016/j.nonrwa.2008.09.010).
- K.V. Prasad, D. Pal, and P.S. Datti. Commun. Non-Linear Sci. Numer. Simulat. **14**, 2178, (2009). doi:[10.1016/j.cnsns.2008.06.021](https://doi.org/10.1016/j.cnsns.2008.06.021).
- K.V. Prasad, K. Vajravelu, and P.S. Datti. Int. J. Thermal Sci. **49**, 603 (2010). doi:[10.1016/j.ijthermalsci.2009.08.005](https://doi.org/10.1016/j.ijthermalsci.2009.08.005).
- N. Ahmed, S.T. Mohyud-Din, and S.M. Hassan. Aerospace Sci. Technol. **48**, 53 (2016). doi:[10.1016/j.ast.2015.10.022](https://doi.org/10.1016/j.ast.2015.10.022).
- U. Kan, N. Ahmed, and S.T. Mohyud-Din. Aerospace Sci. Technol. (2015). doi:[10.1016/j.ast.2015.12.009](https://doi.org/10.1016/j.ast.2015.12.009).
- U. Kan, N. Ahmed, and S.T. Mohyud-Din. Neural Comput. Appl. (2015). doi:[10.1007/s00521-016-2187-x](https://doi.org/10.1007/s00521-016-2187-x).
- S.U.S. Choi. ASME Fluid Eng. Div. **231**, 99 (1995).
- A.M. Rohni, S. Ahmad, and I. Pop. Int. J. Heat Mass Trans. **55**, 1888 (2012). doi:[10.1016/j.ijheatmasstransfer.2011.11.042](https://doi.org/10.1016/j.ijheatmasstransfer.2011.11.042).
- P. Rana and R. Bhargava. Commun. Nonlinear Sci. Numer. Simul. **17**, 212 (2012). doi:[10.1016/j.cnsns.2011.05.009](https://doi.org/10.1016/j.cnsns.2011.05.009).
- N. Aminreza, P. Rashid, and G. Mohamed. Int. J. Thermal Sci. **51**, 1 (2012). doi:[10.1016/j.ijthermalsci.2011.11.017](https://doi.org/10.1016/j.ijthermalsci.2011.11.017).
- M.A.A. Hamad. Int. Commun. Heat Mass Trans. **38**, 487 (2011). doi:[10.1016/j.icheatmasstransfer.2010.12.042](https://doi.org/10.1016/j.icheatmasstransfer.2010.12.042).
- N.A. Yacob, A. Ishak, R. Nazar, and I. Pop. Nanoscale Res. Lett. **6**, 1 (2011). doi:[10.1186/1556-276X-6-314](https://doi.org/10.1186/1556-276X-6-314).
- E.M.A. Elbashbeshy, T.G. Emam, and M.S. Abdel-wahed. Heat Mass Trans. **50**(1), 57 (2014). doi:[10.1007/s00231-013-1224-x](https://doi.org/10.1007/s00231-013-1224-x).
- E.M.A. Elbashbeshy, T.G. Emam, and M.S. Abdel-wahed. Int. J. Appl. Math. **14**(10), 436 (2012).
- A. Alsaedi, M. Awais, and T. Hayat. Commun. Nonlinear Sci. Numer. Simul. **17**, 4210 (2012). doi:[10.1016/j.cnsns.2012.03.008](https://doi.org/10.1016/j.cnsns.2012.03.008).
- E. Magari and A. Pantokratoras. Int. Commun. Heat Mass Trans. **38**, 554 (2011). doi:[10.1016/j.icheatmasstransfer.2011.03.006](https://doi.org/10.1016/j.icheatmasstransfer.2011.03.006).
- T.G. Motsumi and O.D. Makinde. Phys. Scr. **86**, 045003, (2012). doi:[10.1088/0031-8949/86/04/045003](https://doi.org/10.1088/0031-8949/86/04/045003).
- F.M. Hady, F.S. Ibrahim, S.M.A. Gaied, and M.R. Eid. Nanoscale Res. Lett. **7**, 229, (2012). doi:[10.1186/1556-276X-7-229](https://doi.org/10.1186/1556-276X-7-229).
- E.M.A. Elbashbeshy, T.G. Emam, and M.S. Abdel-wahed. Thermal Sci. **19**(5), 1591 (2015). doi:[10.2298/TSCI12007111E](https://doi.org/10.2298/TSCI12007111E).
- A. Pantokratoras and T. Fang. Phys. Scr. **87**, 015703 (2013). doi:[10.1088/0031-8949/87/01/015703](https://doi.org/10.1088/0031-8949/87/01/015703).
- S.T. Mohyud-Din and S.I. Khan. Aerospace Sci. Technol. **48**, 186 (2016). doi:[10.1016/j.ast.2015.10.019](https://doi.org/10.1016/j.ast.2015.10.019).
- U. Khan, N. Ahmed, and S.T. Mohyud-Din. A numerical study. In Neural computing and applications. 2015. doi:[10.1007/s00521-015-2035-4](https://doi.org/10.1007/s00521-015-2035-4).
- M.S. Abdel-wahed and T.G. Emam. Thermal sciences. 2016. doi:[10.2298/TSCI160312218A](https://doi.org/10.2298/TSCI160312218A).
- M.S. Abdel-wahed and M. Akl. AIP Adv. **6**, (2016). doi:[10.1063/1.4962961](https://doi.org/10.1063/1.4962961).
- N. Anbucbezhian, K. Srinivasan, K. Chandrasekaran, and R. Kandasamy. Appl. Math. Mech. **33**, 765 (2012). doi:[10.1007/s10483-012-1585-8](https://doi.org/10.1007/s10483-012-1585-8).
- R. Kandasamy, I. Muhammin, and R. Mohamad. Int. J. Mech. Sci. **70**, 146 (2013). doi:[10.1016/j.ijmecsci.2013.03.007](https://doi.org/10.1016/j.ijmecsci.2013.03.007).
- T. Fang, J. Zhang, and Y. Zhong. Appl. Math. Comput. **218**, 7241 (2012). doi:[10.1016/j.amc.2011.12.094](https://doi.org/10.1016/j.amc.2011.12.094).
- E.M.A Elbashbeshy, T.G. Emam, and M.S. Abdel-wahed. Can. J. Phys. **91**, 699 (2013). doi:[10.1139/cjp-2013-0168](https://doi.org/10.1139/cjp-2013-0168).
- M.S. Abdel-wahed, E.M.A. Elbashbeshy, and T.G. Emam. Appl. Math. Comput. **254**, 49 (2015). doi:[10.1016/j.amc.2014.12.087](https://doi.org/10.1016/j.amc.2014.12.087).

## List of symbols

- |              |   |
|--------------|---|
| $u, v$       | velocity components in the $x$ and $y$ directions, respectively   |
| $\nu$        | kinematic viscosity   |
| $\rho$       | density of the base fluid   |
| $\sigma$     | electrical conductivity   |
| $B(x)$       | strength of the magnetic field  |
| $\alpha^x$   | thermal diffusion   |
| $D_B$        | Brownian diffusion coefficient  |
| $D_T$        | thermophoretic diffusion coefficient  |
| $\rho^*$     | Boltzmann constant  |
| $\alpha^*$   | Rosseland mean absorption   |
| $b$          | constant  |
| $\phi(\eta)$ | dimensionless concentration   |
| $\eta$       | similarity variable   |
| $\psi$       | stream function   |
| $\alpha$     | thickness parameter $\alpha = \delta\sqrt{a/v}$   |
| $\theta_w$   | temperature ratio $\theta_w = T_w/T_\infty$   |
| $Pr$         | Prandtl number $Pr = \nu/\alpha$  |
| $Le$         | Lewis number, $Le = \nu/D_B$  |
| $M$          | magnetic field parameter, $M = \beta_0^2 \sigma / \rho \nu$   |
| $N_b$        | Brownian motion parameter, $N_b = (\tau D_B / \nu)(C_w - C_\infty)$   |
| $N_t$        | thermophoresis parameter, $N_t = (\tau D_t / \nu T_\infty)(T_w - T_\infty)$   |
| $R_d$        | radiation parameter, $R_d = 4\sigma^* T_\infty^3 / \kappa \alpha$   |
| $\tau$       | ratio between the effective heat capacity of the nanoparticles and heat capacity of the fluid, $\tau = (\rho C_p)_p / (\rho C_p)_f$ |